PERGAMON

International Journal of Multiphase Flow 26 (2000) 1117–1140

International Journal of Multiphase Flow

www.elsevier.com/locate/ijmulflow

Flow structure in horizontal oil–water flow

P. Angeli*, G.F. Hewitt

Department of Chemical Engineering, Imperial College of Science, Technology and Medicine, Prince Consort Road, London SW7 2BY, UK

Received 18 November 1998; received in revised form 1 July 1999

Abstract

The flow structure occurring during the cocurrent flow of oil (1.6 mPa s viscosity and 801 kg/m^3 density) and water was investigated using two 1-in. nominal bore horizontal test sections made from stainless steel and acrylic resin respectively. Two methods were used for the flow pattern identification, namely high speed video recording and determination of the local phase fractions with a high frequency impedance probe, while the continuous phase in dispersed flows was recognised with a conductivity needle probe.

Measurements were made for mixture velocities varying from 0.2 to 3.9 m/s and input water volume fractions from 6% to 86%. Over this range of conditions, many different flow patterns were observed, ranging from stratified to fully mixed. Annular flow did not appear. In general, the mixed flow pattern appeared in the steel pipe at lower mixture velocities than in the acrylic pipe, where, also, oil was the continuous phase for a wider range of conditions. The visual observations were consistent with the measurements using the high frequency impedance probe. In certain ranges of conditions the distribution of the phases differed dramatically between the stainless steel and the acrylic pipes. The average in-situ velocity ratios of the two phases in the acrylic pipe calculated from the phase distribution measurements were in general lower than unity.

Keywords: Liquid–liquid; Flow patterns; Stratified flow; Dispersed flow; Local probe; Conductivity probe; Velocity ratio

* Corresponding author. Present address: Department of Chemical Engineering, University College London, Torrington Place, London WC1E 7JE, UK. Tel.: +44-171-419-3832; Fax: +44-171-383-2348.

E-mail address: p.angeli@ucl.ac.uk (P. Angeli).

0301-9322/00/$ - see front matter
PII: S0301-9322(99)00081-6

1. Introduction

Liquid–liquid flows appear in many industrial processes and in the petroleum industry in particular, where oil and water are often produced and transported together. During their cocurrent flow in a pipe the deformable interfaces of the two fluids can acquire a variety of characteristic distributions which are called *flow regimes* or *flow patterns*. The interest on the flow patterns lies on the fact that in each regime the flow has certain hydrodynamic characteristics. When flow patterns are taken into account, more accurate models can be developed for two-phase flows.

Clearly the flow patterns would be expected to be determined (for a given pipe diameter and orientation) by the velocities, the volume fractions and physical properties (density and viscosity) of the respective phases. A further parameter is also likely to be important, namely the wetting characteristics of the tube wall. Wetting effects can be important in gas–liquid flows (for instance when the channel wall is hydrophobic in air–water flow) but are not usually taken into account. However, with liquid–liquid flows, the experiments described here show that differences due to the wall are potentially very significant. Most laboratory experiments on liquid–liquid flows have been carried out with acrylic resin tubes. On the other hand in most applications (oil-water pipelines, etc.) the pipes are constructed from steel. Comparison of the pressure gradients in acrylic and stainless steel tubes for identical conditions (Angeli, 1996; Angeli and Hewitt, 1998) revealed substantial differences in values obtained for the respective wall materials. The objective of the work described here was to explore the flow structure (flow pattern and phase distribution in a pipe cross section) for the different wall materials.

Using a high speed video camera, flow patterns were recorded for a wide range of flowrates in two test sections made from acrylic resin and stainless steel respectively. In addition to video recording, a high frequency impedance probe and a conductivity probe were also used for measuring phase distribution and identifying the continuous phase respectively. In what follows, Section 2 briefly describes the available literature on liquid–liquid flow patterns while Section 3 refers to the experimental system and the different experimental techniques used for flow pattern identification. Section 4 describes the flow patterns observed and the hold up measurements obtained from the high frequency probe. Finally, Section 5 summarises the conclusions.

2. Literature

2.1. Flow patterns

Although in gas–liquid flows extensive studies have been carried out on flow pattern boundaries for a wide range of fluid properties, and in some cases models have been proposed that can predict the transition from one flow pattern to the other, in liquid–liquid flows the amount of available data on flow patterns is still small. The main flow regimes that have been observed in horizontal liquid–liquid flows may be classified as follows:

Stratified flow: here the two fluids flow in separate layers according to their different densities.

Annular flow: here one fluid forms an annular film on the pipe wall and the other flows in the pipe centre. This flow regime is common when the two liquids have equal densities or when one liquid has large viscosity.

Dispersed flow: here one fluid is continuous and the other is in the form of drops dispersed in it.

In Table 1 a summary of the experimental studies on flow patterns in horizontal oil–water pipe flow is presented. These studies led to the generation of flow pattern maps which, however, show considerable variations. Apart from the obvious influence of phase superficial velocities and channel diameter, the variables which were also found to influence the flow patterns were:

1. *Density difference*: Most of the studies were carried out with significant density difference between the phases. For the horizontal pipes used in the studies listed in the above table, this led to asymmetries in the flow with the heavier phase tending to flow near the bottom of the tube. However, Charles et al. (1961) used oils with the same density as water; in this case the flow patterns observed were symmetrical and annular flow also appeared.
2. *Oil viscosity*: When the flow pattern is dispersed and when water is the continuous phase, the oil viscosity has little effect on the flow behaviour (Arirachakaran et al., 1989). The oil viscosity has a profound influence on the occurrence of annular flows when there is density difference between the phases; annular flow with water forming the annulus adjacent to the tube wall seems to occur only with oils with very high viscosity. Annular flow with the oil phase flowing adjacent to the tube wall seems to occur only with oils of intermediate

Table 1
Experimental studies on flow pattern maps during horizontal oil–water flows

Authors	Pipe ID	Pipe material	Oil properties	
			Viscosity (mPa s)	Density (kg/m^3)
Russel et al. (1959)	25.4 mm	Cellulose acetate-butyrate	18	834
Charles et al. (1961)	26.4 mm	Cellulose acetate-butyrate	6.29, 16.8, 65.0	0.998
Hasson et al. (1970)	12.6 mm	Glass hydrophilic (cleaned) and hydrophobic (treated)	1	1020
Guzhov et al. (1973)	39.4 mm	N/A	21.7	896
Arirachakaran et al. (1989)	41.1 mm	Steel	84 (in the provided flow pattern map; flow patterns also observed for oil viscosities 4.7, 58, 115)	867 (oils with densities 867–898 also used)
Nädler and Mewes (1995)	59.0 mm	Acrylic (perspex)	20	841
Trallero (1995)	50.0 mm	Acrylic	29	884
Valle and Kvandal (1995)	37.5 mm	Glass	2.3	794

viscosities, while when the oil has low viscosity this flow pattern is consumed by the oil continuous dispersed flow patterns (Guzhov et al., 1973; Arirachakaran et al., 1989).

3. *Wetting properties of the wall*: One of the main phenomena explored in the present work is the influence of the wall material on flow behaviour. The existence of wall wetting effects was suggested by Charles et al. (1961) as the source of the different behaviour between the high and low viscosity oils used in his experiments. Hasson et al. (1970), who experimented with oil–water mixtures with equal densities, suggested that wall wetting effects were important in the annular core break-up mechanism and in the transition from annular flow to other flow regimes. However it is believed that the present experiments are the first in which such effects have been investigated in detail in the normal range of fluid densities and flow patterns.

In addition to the experimental studies of flow patterns summarised above, criteria on flow pattern transition have been given by Brauner and Moalem Maron (1992) (for stratified, stratified dispersed, annular, slug and dispersed flow regimes) and Trallero (1995) (for separated, oil dominated and water dominated dispersed flow regimes).

2.1.1. Methods of flow pattern identification

The most common way to identify the different flow patterns is to observe the flow in a transparent channel or through a transparent window on the pipe wall. As an extension to visual observation, photographic or video techniques have also been widely used; for very rapid phenomena, high speed photography or video is necessary. However, even high speed photography/video is often not sufficient to give a clear delineation of the flow pattern, since complex interfacial structures result in multiple reflections and refractions that obscure the view, especially in the centre of the pipe and at high flow velocities. In addition photographic/video techniques usually record the flow from outside the pipe, close to the pipe wall, which can be misleading especially close to the flow pattern boundaries, where the visual differences between two flow patterns can be very small. As a result, in gas-liquid flows, a variety of other techniques has been used to supplement the visual observations. A review of these is given by Hewitt (1978). In liquid–liquid flows on the contrary, investigators have almost exclusively used visual observation and photography related techniques (Russell et al., 1959; Charles et al., 1961; Hasson et al., 1970; Arirachakaran et al., 1989). However, it is worth noting that Nädler and Mewes (1995) reported the use of a conductivity probe to identify the continuous phase in the dispersed region, and that Vigneaux et al. (1988) used an impedance probe to obtain phase distribution in inclined oil–water pipeline flow. The use of local probes to give the volume fraction distribution over a pipe cross section can also indicate the different flow patterns and thus supplement visual observation.

3. Experimental set up

The flow patterns formed during the simultaneous pipeline flow of oil and water, were observed in the pilot scale liquid–liquid flow facility shown in Fig. 1, which is described in detail by Angeli (1996). Water and oil were metered and supplied separately from two storage

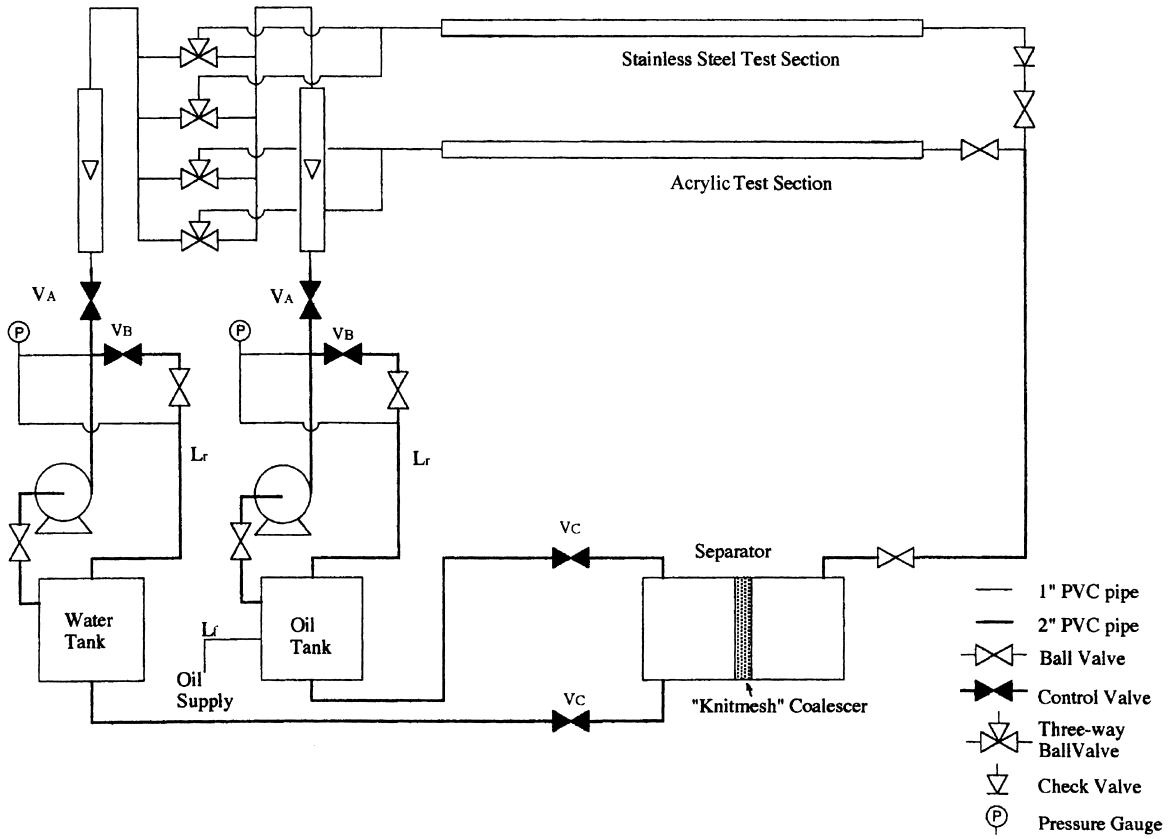

Fig. 1. Liquid–liquid flow facility.

tanks to either one of two test sections made from stainless steel and Transpalite^{TM} (a type of acrylic resin). The steel pipe has 24.3 mm ID and 9.7 m total length and the acrylic pipe has 24 mm ID and 9.5 m total length. The water was introduced at the end of the respective tube and the oil through a T-junction at the bottom of the tube about 15 cm downstream from the end of the tube. The mixture of the two fluids, after the test sections, is separated in a horizontal liquid–liquid separation vessel with 1.94 m length and 0.54 m ID, equipped internally with a Knitmesh^{TM} coalescer. The coalescer, designed to accelerate the separation process of the two liquids, consists of filaments of two different materials, metal and plastic, with different wetting properties, "knitted" together. The fluids used in the present work were tap water and kerosene (EXXOL D80), with properties shown in Table 2. The flowrates of the fluids were measured with variable area flowmeters, calibrated for the appropriate fluid with an accuracy of $\pm 1\%$ of the maximum flowrate.

Two different pipes were used in order to examine the effect of the wall material on the flow phenomena. The steel pipe is rougher (7×10^{-5} m roughness) than the acrylic pipe (1×10^{-5} m roughness); the acrylic pipe is also preferentially wetted by oil (Valle, 1995).

All the experiments were performed about 9 m from the beginning of both test sections.

Table 2
Oil properties at 20°C

Product Name	EXXSOL D80
Density	801 kg/m^3
Viscosity	1.6 mPa s
Interfacial tension air–oil	0.027 N/m
Interfacial tension oil–water	0.017 N/m

Apart from video recording two types of probes assisted the flow pattern identification in the present work. The different techniques are described below.

3.1. Video recording

Flow patterns were recorded using a high speed videocamera (Hadland Photonics High Speed Videoscope), while light was provided by a stroboscopic Xenon Light, synchronised to the camera. The Videoscope has a filming rate of 50 Hz, while the stroboscopic light has a 20 μs duration. The flow patterns for each test condition were recorded and could be observed later in slow motion. In the stainless steel pipe a short transparent acrylic pipe, 10 cm long, which could be placed between two flanges, was used for the recording. Proper illumination was necessary in order to obtain good quality pictures. It was found that best results were obtained when the light was illuminating the pipe from the back opposite to the camera lens, through a thin porous paper.

3.2. High frequency impedance probe

A local probe is a point sensor, whose shape is usually similar to that of a needle. The probe emits a two-state signal indicating which phase surrounds a sensing part of the tip, based on the detection of differences between the physical properties of the two phases. From the fraction of the time that the probe resides in a given phase, the local volume fraction of that phase can be derived. In the two-phase example shown in Fig. 2 the local volume fraction $\varepsilon_k(x)$ of phase k at a point x inside the pipe is:

$$\varepsilon_k(x) = \lim_{T\to\infty} \sum_i \frac{T_{ki}}{T} \tag{1}$$

where T_k is the time the probe indicates phase k and T is the total time of the experiment.

Local probes may discriminate between the phases based on a variety of properties (thermal conductivity, refractive index, electrical resistance or electrolytic current). Due to the large differences in electrical properties between oil and water, from the variety of local probes, the electrical impedance ones, which are sensitive to the differences in complex resistance (impedance) of the phases, are suitable for oil–water flows (Cartellier and Achard, 1991). The probe signal is provided by the voltage differences registered from both sides of an external resistance. Various probe excitation methods have been investigated. For direct current

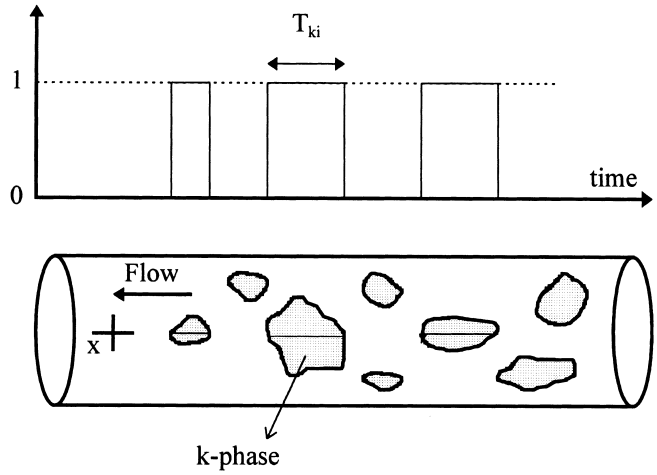

Fig. 2. Local probe response in a two-phase flow (as in Cartellier and Achard, 1991).

excitation, which is easy to set up and is the least expensive technique, the measurement relies on the resistivity variation. However, polarisation effects as well as electrochemical attack often induce accelerated degradation of the sensitivity of the probe response (Jones and Delhaye, 1976). Moreover the liquid resistivity is a function of the temperature and of any liquid impurities, resulting in uncertainties in the measure of the volume fraction. With an alternating current excitation of moderate frequency, the measurement is still based on the resistivity but the limitations of the probe due to polarisation and electrolysis phenomena are avoided (Teyssedou et al., 1988); however the other sources of error connected to liquid resistivity still remain. Alternating current excitation at higher frequencies can overcome these problems, since the capacitance of the phases becomes the most sensitive parameter (Cartellier and Achard, 1991). High frequency impedance probes are particularly suitable for oil–water flow measurements because of the large dielectric constant contrast between the two liquids (Vigneaux et al., 1988).

In the light of the above considerations, an alternating current high frequency (1 GHz) impedance probe, that had been developed by Schlumberger Cambridge Research, was chosen as the most suitable for the oil–water two phase flow experiments performed here. The probe tip and mounting are illustrated in Fig. 3. The probe gives a two level signal, where the lower level represents the oil and the higher the water phase. The sensitive probe tip consists of two conductors separated by a PTFE insulator tube with 0.66 mm nominal outer diameter. The inner conductor is a silver-plated, copper-clad steel wire with 0.203 mm nominal diameter and the outer conductor is an oxygen-free copper tube with 0.86 mm nominal outer diameter. The probe tip, which is shown in Fig. 3a, has this particular shape in order to achieve immediate piercing of the interface with little deformation at the moment of contact. This configuration has also been shown to give clearer response. The probe forms part of a Wheatstone bridge with a reference probe in the air. Alternating current at 1 GHz was used for the probe excitation. The probe traversing mechanism, which allows the probe tip to scan a pipe diameter, and the technique used for mounting the probe in the pipe are shown in Fig. 3b.

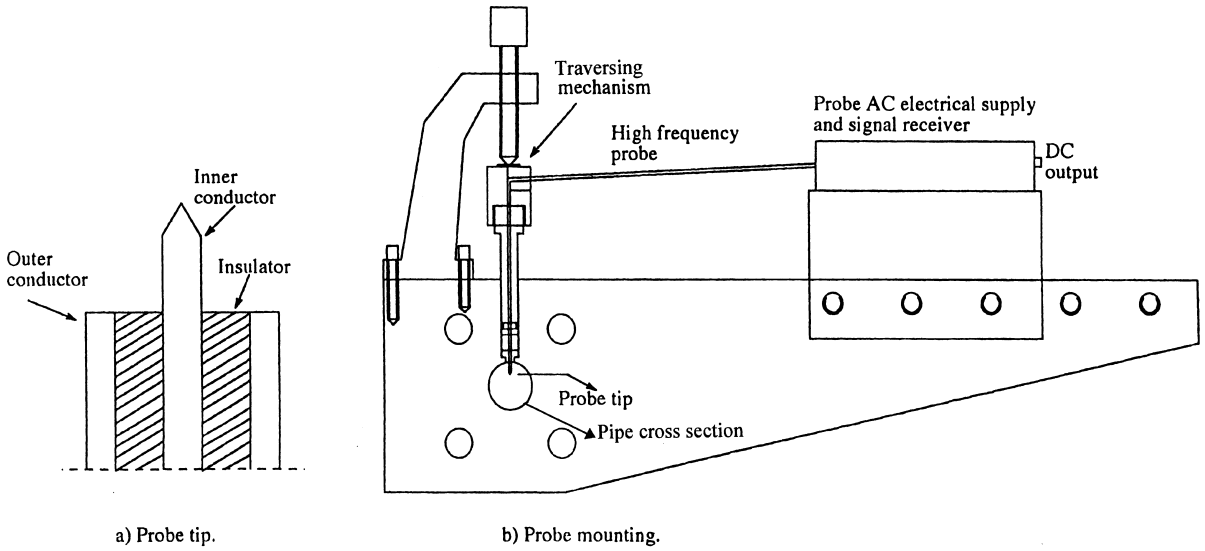

Fig. 3. High frequency impedance probe. (a) Probe tip. (b) Probe mounting.

This particular mounting allows the probe to be traversed along a diameter at any angle through the tube axis and the probe can be placed between any pair of flanges in the test section.

Data was collected every 2 mm along three pipe diameters with angles 0°, 45° and 90° from a horizontal plane. Close to the pipe walls the distance between the data collecting points was 1 mm, since this could show which phase was actually in contact with the pipe wall. Data was collected with a frequency of 5000 Hz over a period of 12 s. Some initial experiments, performed over different periods of time, showed that variations of the local volume fraction due to flow fluctuations were adequately averaged over the period of 12 s.

3.2.1. Signal processing method

Several factors result in the departure of the probe signal from the ideal square wave form shown in Fig. 2, where the two levels represent contact of the probe tip with each respective phase. There is usually a delay between the time the probe tip comes in contact with a phase and the time the probe signal takes its final value for this phase. This delay could be due to the time this phase needs to wet the whole probe tip (depending on wetting/dewetting phenomena), and/or, in an electrical probe, to the delayed response of the electronic circuit. Also in the dispersed region, since the probe tip can only have a finite size, there may be drops smaller than that size, in which case the signal may not reach the corresponding level for the dispersed phase and will not have a square wave form. A suitable signal processing technique is therefore necessary to extract the required information from the raw signal. The most commonly used method for processing the signal is the so-called "threshold" technique, where the intersection of the raw signal $S(t)$ with set level(s) is used to determine the start and end of the equivalent rectangular wave. However, the optimum threshold level(s) can depend on the phase volume

fraction (Kobori and Terada, 1978; Teyssedou et al., 1988). Furthermore, signals which do not reach the set level(s) go undetected.

Some investigators (Burgess and Calderbank, 1975; Cartellier and Achard, 1991) tried to accurately locate on the raw signal the contact point of the probe tip and the interface. Their results, obtained from gas–liquid experiments, showed that the contacts are related to the very beginning of the signal rise or fall. A method that attributes the change in the slope of the signal to the beginning of a phase is therefore needed. In this way very small contributions can be detected, which result either from high velocities where the passing time of a phase is shorter than the delay time, or, in dispersed flow, from drops smaller than the size of the probe tip.

In the present work, a signal processing technique based on a method proposed by van Der Welle (1985) was used. This technique detects the beginning of the rise or the fall of a signal, and then transforms the raw signal into a rectangular wave taking as a starting point the change in the signal slope. The main idea is that each sample of the signal is compared with two self-adjusting trigger levels and its implementation is summarised in Table 3. The signal amplitude α_n of the n^{th} sample is compared with the amplitude α_{n-1} of the previous sample and with two adjustable maximum and minimum values, $\alpha_{\max}$ and $\alpha_{\min}$ respectively. In the beginning two initial values for $\alpha_{\max}$ and $\alpha_{\min}$ are given. If α_n is greater than α_{n-1} then the maximum $\alpha_{\max}$ is changed and is set equal to α_n. If α_n and α_{n-1} are equal then there is no change in the maximum and the minimum values, and if α_n is lower than α_{n-1} then the minimum changes and is set equal to α_n. The amplitude α_n is then compared with the new maximum and minimum values; in this comparison the margin x (signal "clip" level) accounts for the signal noise. If Eq. (2)

$$\alpha_n > \alpha_{\min} + x \tag{2}$$

is true then the output is 1 (which represents the water phase), while if Eq. (3)

$$\alpha_n < \alpha_{\max} - x \tag{3}$$

is true then the output is 0 (which represents the oil phase). If neither Eq. (2) nor Eq. (3) is true then the previous value (1 or 0) is kept. The whole signal is thus converted in a series of 1's and 0's, which represent each one of the two phases. The method assumes that the

Table 3
Implementation of the method proposed by van Der Welle (1985) for processing the signal of a local probe

Condition	Minimum	Maximum	Output
$\alpha_n > \alpha_{n-1}$	q[a]	$\alpha_{\max} = \alpha_n$	
$\alpha_n = \alpha_{n-1}$	q	q	
$\alpha_n < \alpha_{n-1}$	$\alpha_{\min} = \alpha_n$	q	
$\alpha_n > \alpha_{\min} + x$, Eq. (2)			1
$\alpha_n < \alpha_{\max} - x$, Eq. (3)			0
if none of Eq. (2) and (3) true			q

[a] q: no change.

beginning of the change in the signal slope represents the interaction of the probe with the liquid–liquid interface. A FORTRAN programme was developed to process the probe signal data according to the above method (Angeli, 1996). In Fig. 4 the initial signal from the probe is shown together with the same signal in square wave form, after it has been processed.

The distribution of the volume fraction in a pipe cross section could be converted into contour diagrams by using the software program MATHEMATICA. From the local volume fraction measurements of a phase at different points in a pipe cross section, the average cross sectional in-situ volume fraction of this phase can be estimated by integration over the whole pipe cross section. For example the cross sectional average oil volume fraction ε_0 can be evaluated from the following equation:

$$\varepsilon_o = \frac{1}{A}\int_0^A \varepsilon'_o \mathrm{d}A = \frac{1}{A}\sum_i \varepsilon'_{oi} A_i, \text{ and } \sum_i A_i = A \tag{4}$$

where, ε'_{oi} is the local oil volume fraction at a point i in a pipe cross section, A_i is the area of the pipe cross section surrounding point i, and A is the pipe cross sectional area.

During the signal processing there may also be other sources of error resulting from the distortion of the liquid–liquid interface as the probe tip approaches it (Cartellier and Achard,

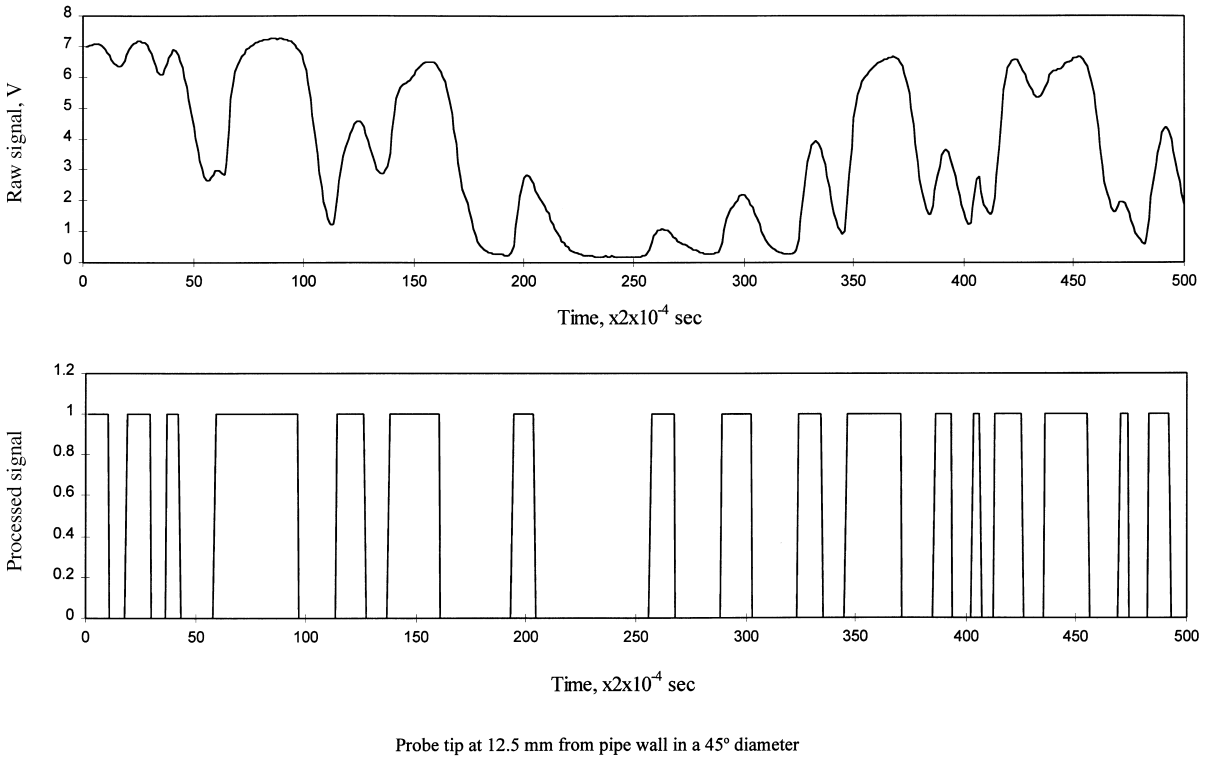

Fig. 4. Raw and processed signal (in square wave form) from the high frequency probe for mixture velocity 1.3 m/s and input oil volume fraction 50% in the acrylic pipe.

1991). It is necessary therefore to validate the performance of the probe by comparison with another method. In the present work the results of the impedance probe compared well with those derived from a displaced needle, two-point conductivity method (Angeli, 1996) for the region where both probes where applicable.

3.3. Conductivity needle probe

In the dispersed flow regime the continuous phase is not readily identified. In the present work since one phase (water) was conductive and the other (oil) non-conductive a conductivity probe was used to ascertain phase continuity (Angeli, 1996). The probe consists of two copper needles insulated with enamel leaving only a tip free. The needles are mounted in line in the test tube normal to the direction of flow. The needles can move relative to each other while their exact positioning is determined by a micrometer. When an electric current is applied to the needles then there will be a voltage output when the needles are immersed in water and no signal when the needles are immersed in oil. In a water continuous flow there is always a signal no matter how far apart the needles are. On the other hand in an oil continuous flow, when the needles are placed close to each other, there are discrete peaks in the signal indicating contact of the needles with water drops. These peaks disappear when the needles are moved further apart, to a distance larger than the maximum drop size in the dispersion.

For the flow pattern identification the high speed videocamera was mainly used. Experiments were carried out in both pipes for mixture velocities ranging from 0.2 to 3.9 m/s and input water volume fractions ranging from 6% to 86%. The high frequency impedance probe was used for mixture velocities from 1.3 to 1.7 m/s and input oil volume fractions from 25% to 85%. These conditions were chosen because, as it was revealed from the video recording, they represented cases in the boundaries between different dispersed flow regions, which due to the high mixture velocities were difficult to be identified visually. These experiments were done mainly in the acrylic pipe with a smaller range of experiments in the steel pipe, for comparison purposes.

4. Results

4.1. Flow patterns

The main flow patterns which were observed in both the steel and the acrylic pipes are presented below in the order they appeared with increasing mixture velocity and are shown in Figs. 5–8, while the resulting flow pattern maps for the different mixture velocities and input water volume fractions are presented in Figs. 9 and 10 for the steel and the acrylic pipe respectively.

Stratified Wavy flow pattern (SW): here the two fluids flowed in separate layers on the top and the bottom of the pipe according to their densities and their interface was disturbed. This flow pattern existed over a higher range of conditions in the acrylic (mixture velocities up to 0.6 m/s, Fig. 10) than in the steel pipe (mixture velocities up to 0.3 m/s, Fig. 9).

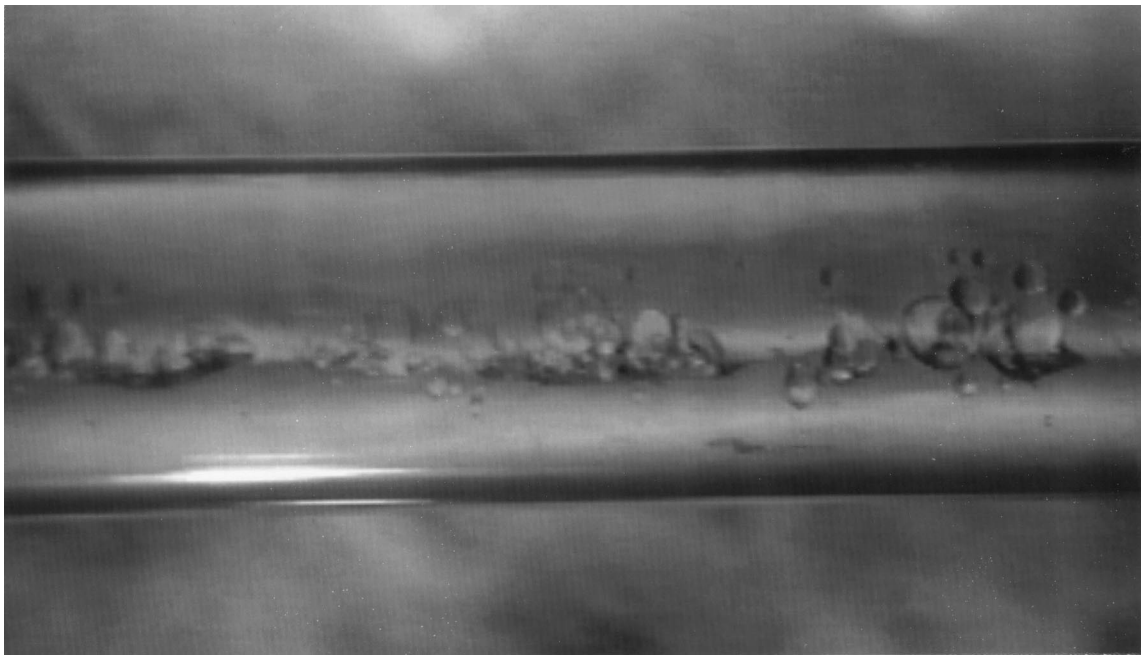

Fig. 5. Stratified Wavy with Drops (SWD) flow pattern in the acrylic pipe.

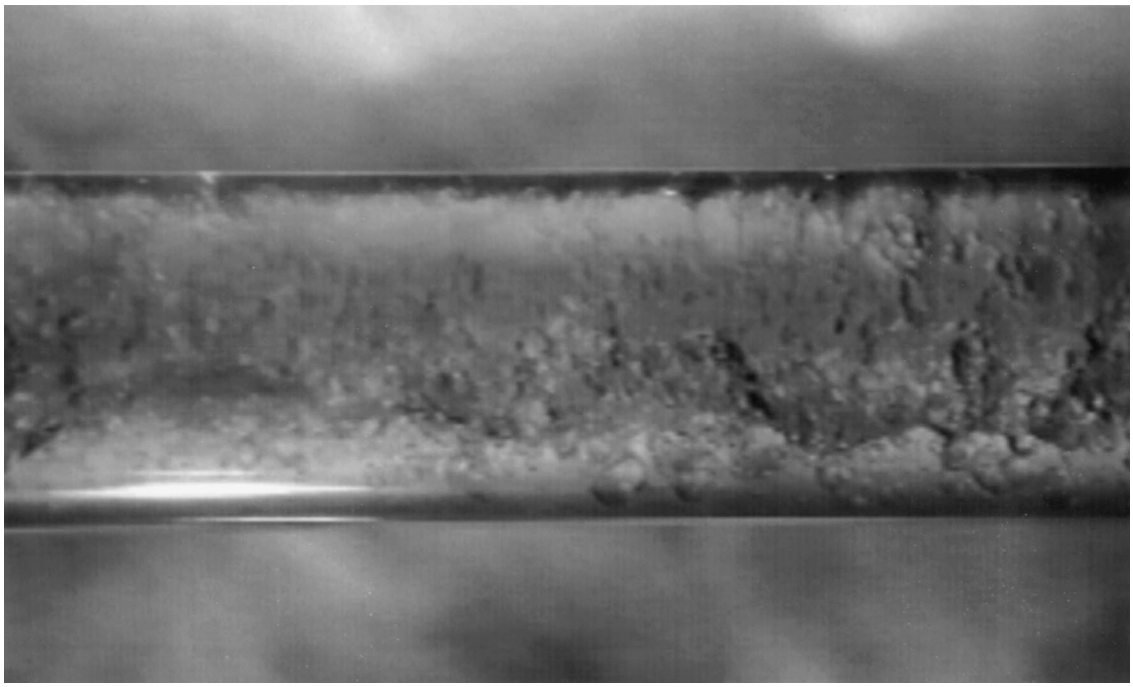

Fig. 6. Three Layer (3L) flow pattern in the acrylic pipe.

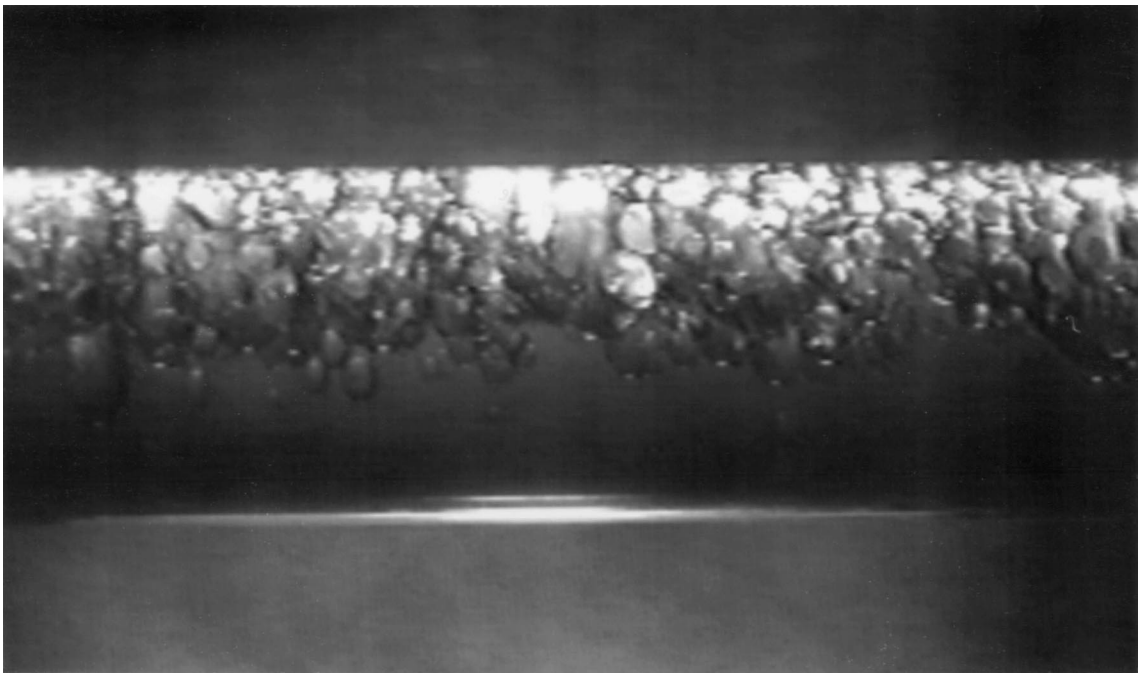

Fig. 7. Stratified Mixed with water layer (SM/water) flow pattern in the acrylic pipe.

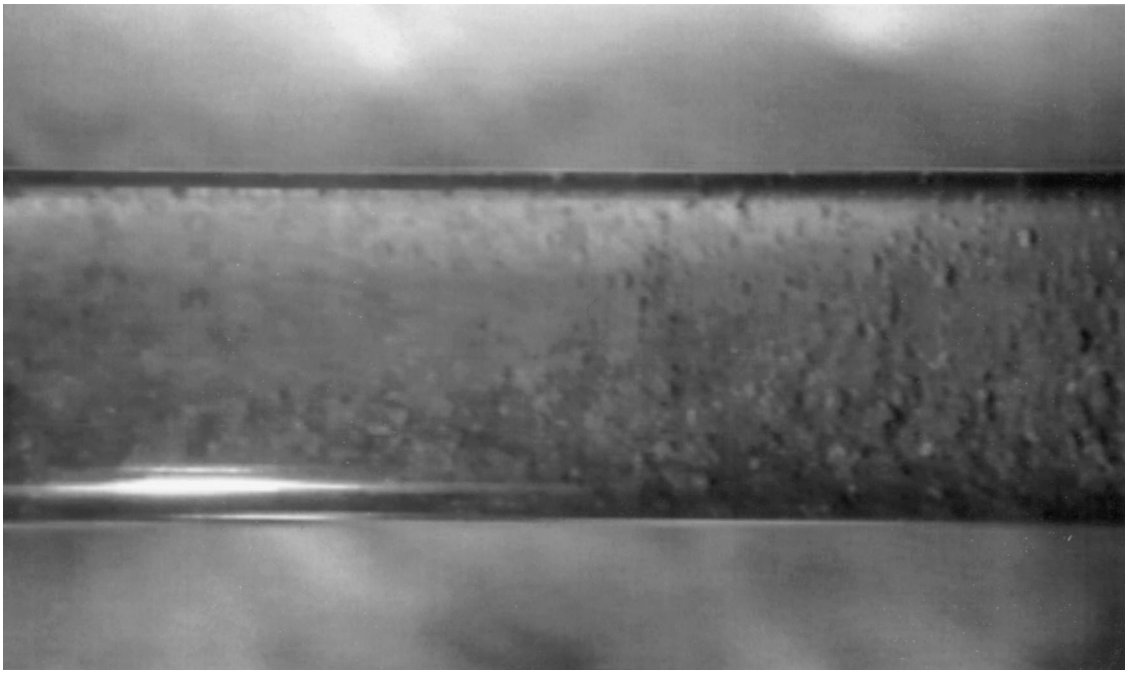

Fig. 8. Mixed (M) flow pattern in the acrylic pipe.

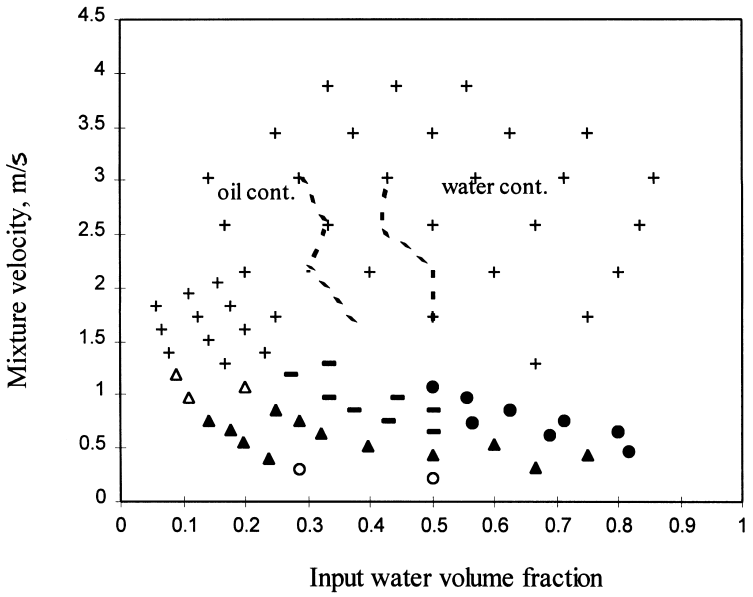

Fig. 9. Flow patterns in the stainless steel test section. ○, stratified wavy (SW); ▬, three layers (3L); △, stratified mixed/oil (SM/oil); - - -, phase continuity boudaries; ▲, stratified wavy/drops (SWD); ●, stratified mixed/water (SM/water); +, mixed (M).

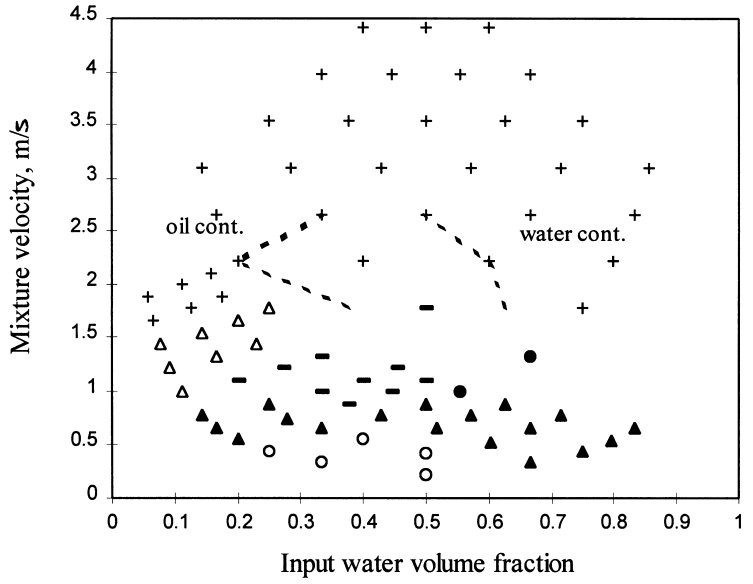

Fig. 10. Flow patterns in the acrylic test section. ○, stratified wavy (SW); ▬, three layers (3L); △, stratified mixed/oil (SM/oil); - - -, phase continuity boudaries; ▲, stratified wavy/drops (SWD); ●, stratified mixed/water (SM/water); +, mixed (M).

As the mixture velocity increased drops appeared at the interface region and the flow pattern became **Stratified Wavy with Drops (SWD)** (see Fig. 5).

Three Layer flow pattern (3L): here there were distinct continuous layers of oil and water at the top and bottom of the pipe respectively but in the interface there existed a layer of drops, while drops of each phase could appear within the other phase (see Fig. 6). This regime appeared at lower mixture velocities in the steel (between mixture velocities 0.7–1.3 m/s and water volume fractions 0.3–0.5, Fig. 9) than in the acrylic pipe (between mixture velocities 0.9 and 1.7 m/s and volume fractions 0.2–0.5, Fig. 10).

Stratified Mixed flow pattern (SM): here one phase was continuous while the other was in the form of drops occupying only part of the pipe. At high water fractions, where water was the continuous phase, there was a layer of oil drops at the top of the pipe (SM/water flow pattern, Fig. 7), while at low water fractions, where oil was the continuous phase, there was a layer of water drops on the bottom of the pipe (SM/oil flow pattern). While the SM/water regime prevailed over a wider range of conditions in the steel than in the acrylic pipe, the opposite happened for the SM/oil regime. Stratified Mixed flow appeared at approximately the same mixture velocities as the three layer and at water volume fractions below 0.3 and above 0.5 in both pipes (Figs. 9 and 10).

Fully Dispersed or Mixed flow pattern (M): here one phase is dispersed more or less uniformly into the other and occupies a whole pipe cross section (see Fig. 8). This flow pattern appeared at mixture velocities higher than 1.3 m/s in the steel tube (Fig. 9) and 1.7 m/s in the acrylic tube (Fig. 10). At low water fractions oil is the continuous phase while at high water fractions water is the continuous phase. In Figs. 9 and 10 the dotted lines indicate the limits of the respective phase continuity. To the left of the left-most line oil was the continuous phase and to the right of the right-most line water was the continuous phase. Results from the conductivity needle probe showed that the change from one phase being continuous to the other (*phase inversion*) is not instantaneous. On the contrary there existed an intermediate flow pattern where both phases were periodically continuous in waves. It is possible that between the two dispersed regimes a stratification of the flow happens. This undefined region is included between the dotted lines in Figs. 9 and 10.

Although the same sequence of flow patterns was observed in both pipes there were also some distinct differences between them:

1. The flow patterns in the steel pipe were in general more disturbed than those in the acrylic pipe. As a result there was only a very narrow Stratified Wavy region in the steel tube while the Mixed region started at lower velocities than in the acrylic tube. This could be due to the different roughness of the two pipes; the higher roughness of the steel pipe compared to that of the acrylic could result for the same flow velocities to a higher degree of turbulence and more disturbed flow patterns.
2. In the acrylic pipe the oil continuous flow regimes (Stratified Mixed/oil, Three Layer) persisted over a wider range of mixture velocities and water fractions than in the steel pipe. One possible explanation is the different wettability of the two pipe materials from the oil and the water. Since oil preferentially wets the acrylic, this could have caused the oil phase to remain continuous over a wider range of conditions in this pipe.

The properties of the pipe wall (roughness and wettability) can therefore affect the flow

patterns and subsequently the pressure gradients, which depend on the flow regime (Angeli and Hewitt, 1998).

4.2. Comparison with other maps

The literature review showed that there is no generalised flow pattern map for the horizontal flow of two immiscible liquids. Thus, the experimental flow pattern maps from both test sections will be compared with the maps given by Arirachakaran et al. (1989) and Nädler and Mewes (1995), since these were observed in pipes similar (in size and material) to those used here. From the published flow pattern maps only the one produced by Valle and Kvandal (1995) was for the same oil as the one used in the present study. Their experiments though were performed in a glass pipe and only covered a small area of stratified flows.

The flow pattern map proposed by Arirachakaran et al. (1989) for flow in a steel pipe is compared with the data from the stainless steel and the acrylic pipes in Fig. 11a and b respectively. In general, Arirachakaran et al. (1989) did not report any flow pattern similar to the Three Layer one, while in the present study no annular flow was observed. It should be noted though that Arirachakaran et al. (1989) also reported that the oil-annulus annular flow pattern did not appear in their experiments with lower viscosity oils, as is the case of the present experiments. The flow regime boundaries in the steel pipe agreed more closely to those given by Arirachakaran et al. (1989) than the ones in the acrylic pipe. This was especially true in the water continuous flows where the Stratified and the Stratified Mixed/water layer patterns appeared in the same range of mixture velocities. The differences between the two maps in Fig. 11a in the oil continuous flows could be due to the different oils that were used in the experiments. The boundaries of the Mixed flow regime however are close to those from Arirachakaran et al. (1989) in both regions of continuity. In the acrylic pipe on the other hand (Fig. 11b) there was a bigger inconsistency between the two flow pattern maps, probably due to the different material of the pipes used. The Stratified regime in the acrylic pipe extended, in the form of Stratified Wavy with Drops pattern, over higher mixture velocities to about 1 m/s, while the Mixed flow started at mixture velocities above the 1 or 1.5 m/s that Arirachakaran et al. (1989) reported.

Nädler and Mewes' (1995) flow pattern map was obtained in a perspex pipe (acrylic resin) and is compared with the flow regimes recorded in the steel and acrylic pipes in Fig. 12a and b respectively. Nädler and Mewes (1995) also did not observe any annular flow pattern but they gave lower mixture velocities as upper limits for the stratified flow than those observed in the present work; especially when compared to the results from the acrylic pipe (Fig. 12b). In addition they did not report a Stratified Mixed/oil regime and their Mixed flow started at mixture velocities below 1 m/s. The interesting aspect of their work is that they reported an undefined region between the oil and the water continuous Dispersed flows, where both phases could be continuous, resembling the Three Layer flow pattern recorded here (regions IIIa and IIIb in Fig. 12).

4.3. Phase distribution

The visual observation of the flow patterns becomes difficult when the mixture velocity

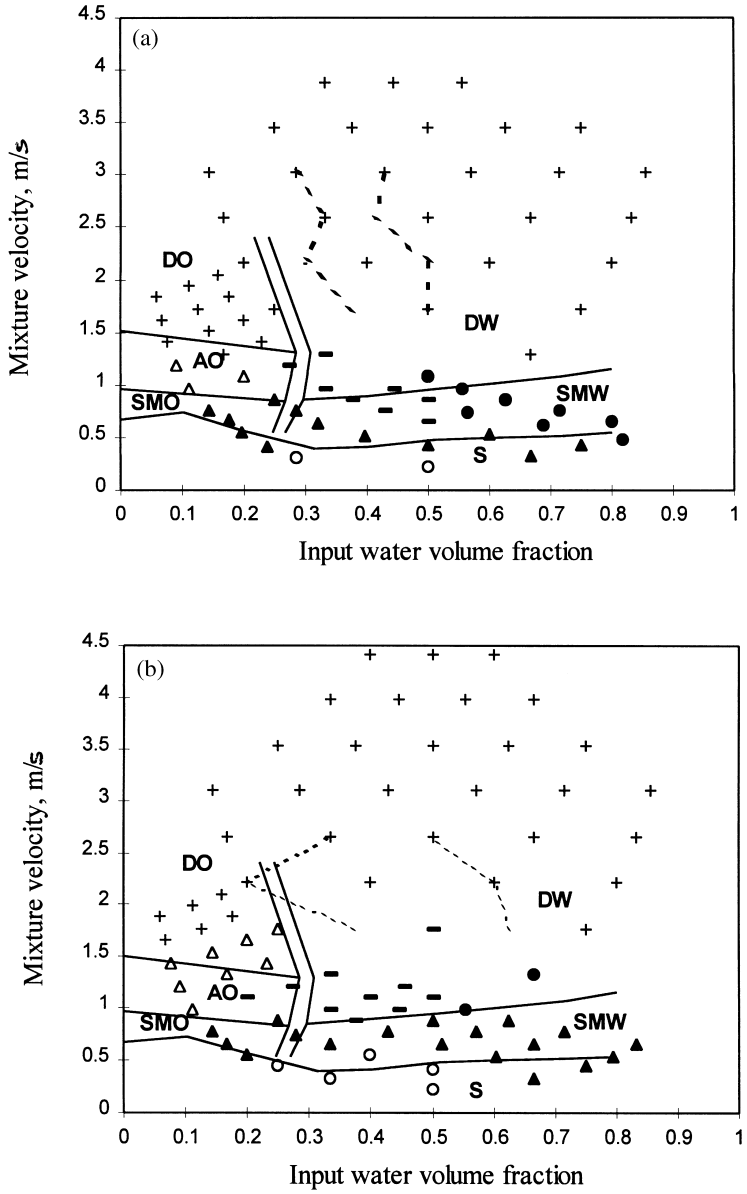

Fig. 11. Comparison of the experimental flow pattern maps with the results from Arirachakaran et al. (1989). (a) Stainless steel pipe. (b) Acrylic pipe. **Regimes defined in the present study:** ○, stratified wavy (SW); ●, stratified mixed/water (SM/water); - - -, phase continuity boudaries; ▲, stratified wavy/drops (SWD); △, stratified mixed/oil (SM/oil); ▬, three layers (3L); +, mixed (M). **Regimes defined by Arirachakaran et al. (1989)**, (boudaries given by continuous lines): S, stratified; SMO, stratified-mixed/oil layer; SMW, stratified-mixed/water layers; AO, annular/oil annulus; DO, mixed-oil cont.; DW, mixed-water cont.

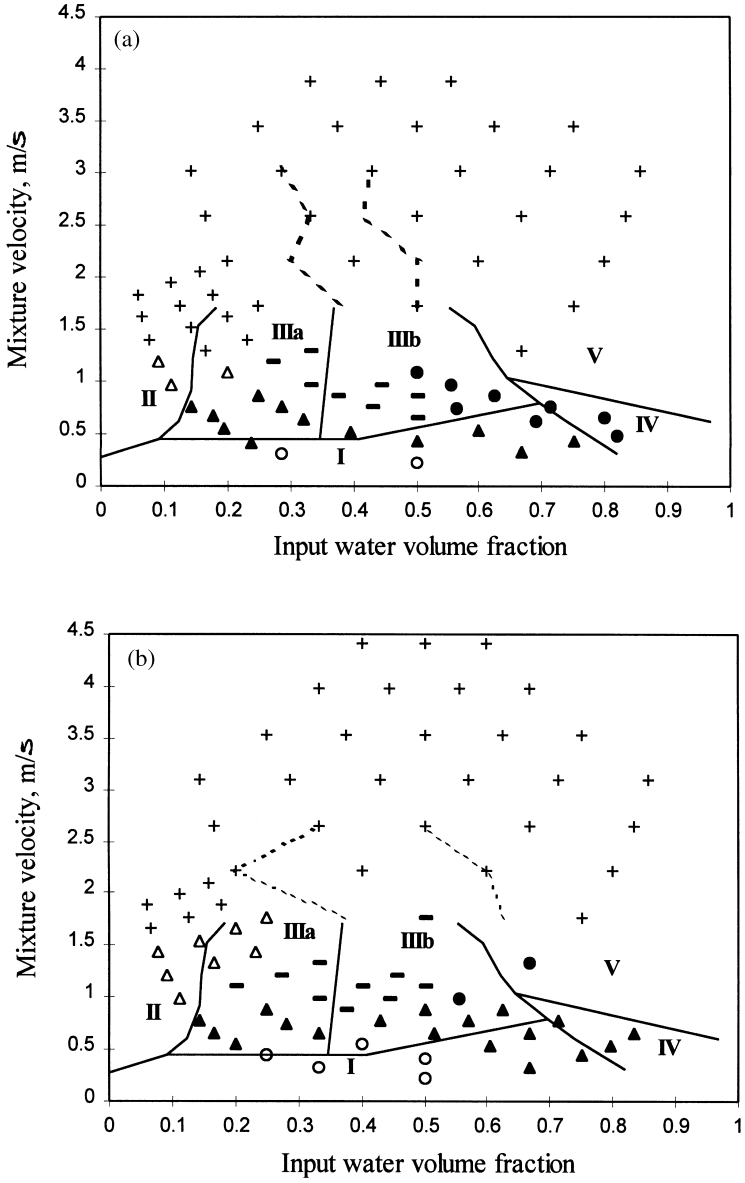

Fig. 12. Comparison of the experimental flow pattern maps with the results from Nädler and Mewes (1995). (a) Stainless steel pipe. (b) Acrylic pipe. **Regimes defined in the present study:** ○, stratified wavy (SW); ●, stratified mixed/water (SM/water); - - -, phase continuity boudaries; ▲, stratified wavy/drops (SWD); △, stratified mixed/oil (SM/oil); ▬, three layers (3L); +, mixed (M). **Regimes defined by Nädler and Mewes (1995)**, (boundaries given by continuous lines): I, statified; II, mixed/oil cont.; IIIa, water-in-oil dispersion and water; IIIb, water-in-oil and oil-in-water dispersions and water; IV, oil-in-water dispersion and water layer; V, mixed/water cont.

increases as the oil–water interface is no longer clear. At these conditions the high frequency impedance probe was used in conjunction with the video recording to clarify certain flow patterns. This clarification was particularly important in distinguishing between the Three Layer, Stratified Mixed and Mixed flow patterns.

In general, the results showed that the phases were more uniformly distributed as the mixture velocity increased. Furthermore the distributions were more homogeneous at low oil fractions than at high ones for the same mixture velocity. Typical results (in this case for the acrylic tube) are shown in Figs. 13 and 14. As can be seen in Fig. 13 for input oil volume fraction 28.5% there is no clear layer of water or oil, and the flow pattern is Three Layer. For the equivalent input water fraction, or 71.5% input oil fraction, shown in Fig. 14, there is a strong volume fraction gradient from the top to the bottom of the pipe and a clear oil layer on top and the flow pattern is Stratified Mixed/oil layer.

Perhaps the most interesting of the results reported here are the comparisons between the acrylic and the steel tubes. Results for oil volume fraction distributions obtained *for exactly the same input flowrates* for the respective tubes are compared in Figs. 15 and 16. The volume fraction distribution has a strong gradient in the acrylic pipe, where the flow pattern is Three Layer, while it is almost uniform in the steel pipe, where the flow pattern is Mixed.

4.4. Hold up

The data for phase distribution measurements were integrated using Eq. (4), giving values of the cross sectional average oil volume fraction ε_o. These may be different from the input ones, since the in-situ average velocities of the phases are not necessarily the same. One way to

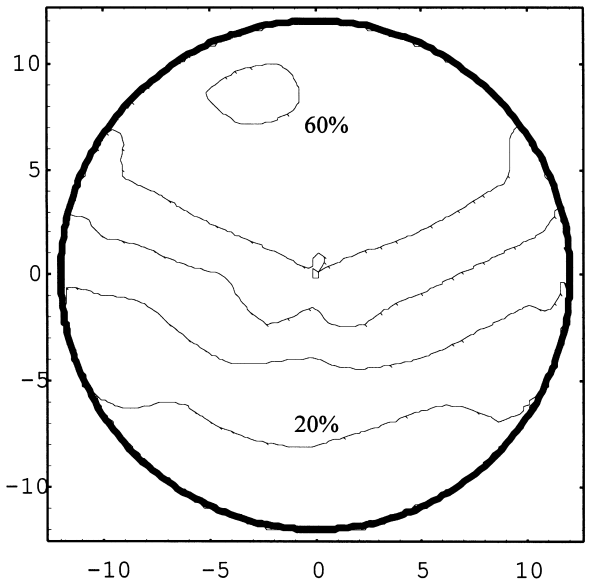

Fig. 13. Oil volume fraction distribution in a cross section in the acrylic pipe for mixture velocity 1.5 m/s and input oil volume fraction 28.5% (Three Layer flow pattern).

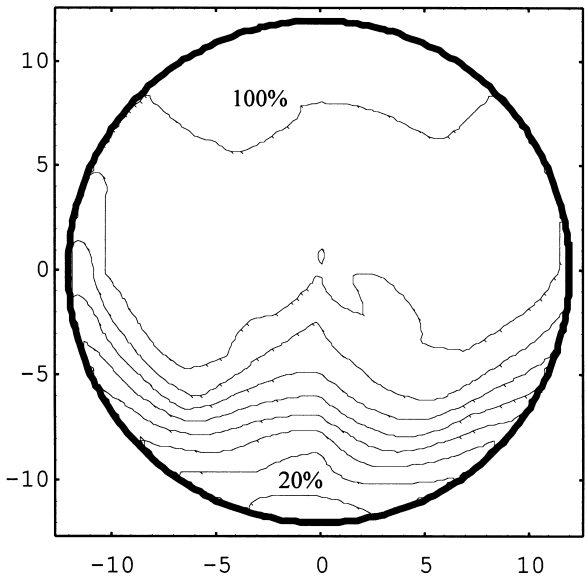

Fig. 14. Oil volume fraction distribution in a cross section in the acrylic pipe for mixture velocity 1.5 m/s and input oil volume fraction 71.5% (Stratified Mixed/oil flow pattern).

express the difference between the in-situ average velocities of the phases is to use their ratio S, which is given by:

$$S = \frac{\beta_o/\beta_w}{\varepsilon_o/\varepsilon_w} \tag{5}$$

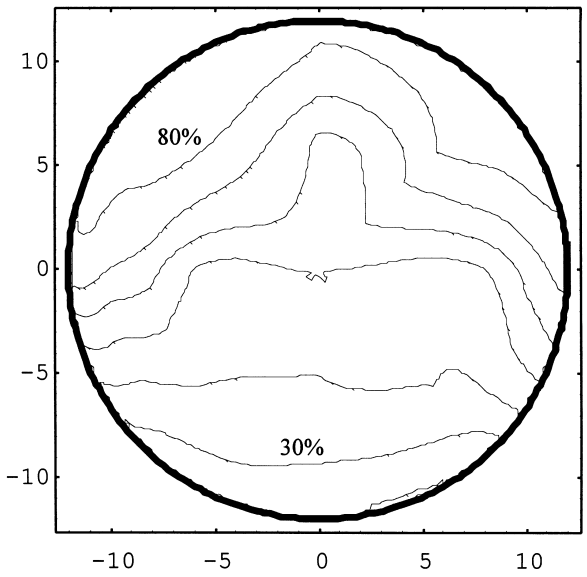

Fig. 15. Oil volume fraction distribution in a cross section in the acrylic pipe for mixture velocity 1.7 m/s and input oil volume fraction 50% (Three Layer flow pattern).

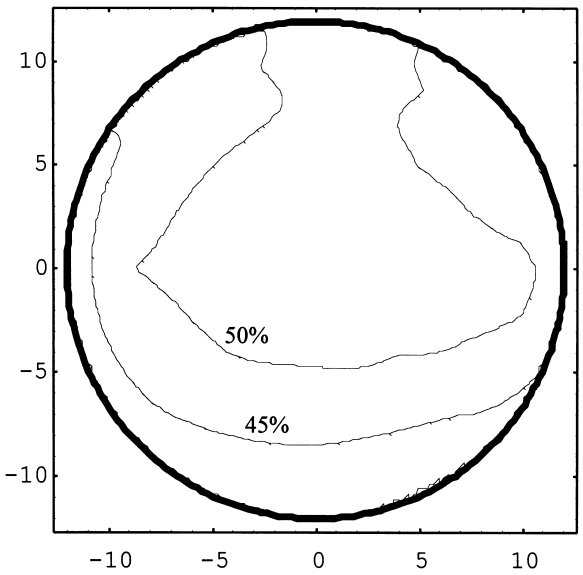

Fig. 16. Oil volume fraction distribution in a cross section in the steel pipe for mixture velocity 1.7 m/s and input oil volume fraction 50% (Mixed flow pattern).

where β_o and β_w are the volume fractions of oil and water in the input flow and ε_o and ε_w are the in-situ volume fractions averaged over the pipe cross section.

The velocity ratios S can be calculated from the phase distribution data in a pipe cross section and for the cases examined in the acrylic pipe are shown in Fig. 17 against the input oil/water volumetric ratio for different superficial water velocities. The velocity ratio in most cases is less than unity, or the in-situ oil/water volume ratio is higher than the input one. In the cases where the velocity ratio was measured, the majority of the flow regimes were Stratified Mixed/oil and Three Layer. In the SM/oil regime the tube wall is totally covered by oil which justifies velocity ratios less than unity. In the Three Layer regime, where both oil and water are in contact with the tube wall, the preferential wetting of the wall by oil may have resulted to higher tube area covered by the oil, which can explain velocity ratios less than unity.

In gas–liquid flows hold up has been correlated empirically with the Lockhart–Martinelli parameter X (Wallis, 1969). The parameter X for oil–water flows can be defined as follows:

$$X^2 = \frac{(\mathrm{d}p/\mathrm{d}z)_o}{(\mathrm{d}p/\mathrm{d}z)_w} \tag{6}$$

and represents the ratio of the pressure gradient of the oil $(\mathrm{d}p/\mathrm{d}z)_o$ flowing alone in the pipeline at the same flowrate as in the two-phase flow, to the pressure gradient of the water $(\mathrm{d}p/\mathrm{d}z)_w$ flowing alone in the pipe at the same flowrate as in the two-phase flow. In this case it is assumed that the more viscous phase, the oil, has substituted the liquid phase and the less viscous one, the water, has substituted the gas phase.

The *two-fluid model* as developed for liquid–liquid flows (Brauner and Moalem Maron, 1989;

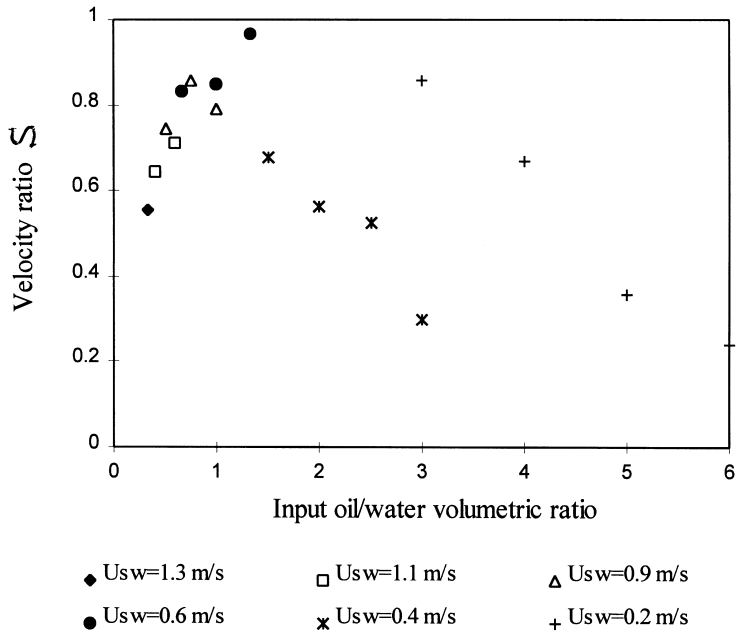

Fig. 17. Velocity ratio in the acrylic pipe for different superficial water velocities.

Kurban et al., 1995) allows the calculation of the in-situ oil volume fraction as a function of the parameter X. The experimental in-situ oil fraction is plotted against X (from Eq. (6)) in Fig. 18. Eq. (7) fits the data with 0.195% relative average error and 6.24 standard deviation of the errors.

$$\ln \varepsilon_o = 0.4134 \ln X - 0.6004 \tag{7}$$

This equation should be regarded as being rather specific to the present data. However, comparison between the equation and the data of Valle and Utvik (1997) for water–oil flows in a 77.9 mm diameter steel pipe demonstrated reasonable agreement. The in-situ oil volume fraction estimated by the two-fluid model is also shown in Fig. 18. As can be seen the two-fluid model underestimates the measurements. This, again, is not surprising since in the two-fluid model the liquids are treated as completely separated layers with a smooth interface. The real physical situation though is not one of complete separation, while the interface between separated layers of the phases is not smooth.

5. Conclusions

New data are presented for flow pattern, phase distribution and phase hold up during liquid–liquid flow in horizontal pipes. The following main conclusions can be drawn from the results obtained:

- The use of a high frequency impedance probe to determine phase distribution together with a double needle probe to establish which of the liquids is the continuous phase, has proved

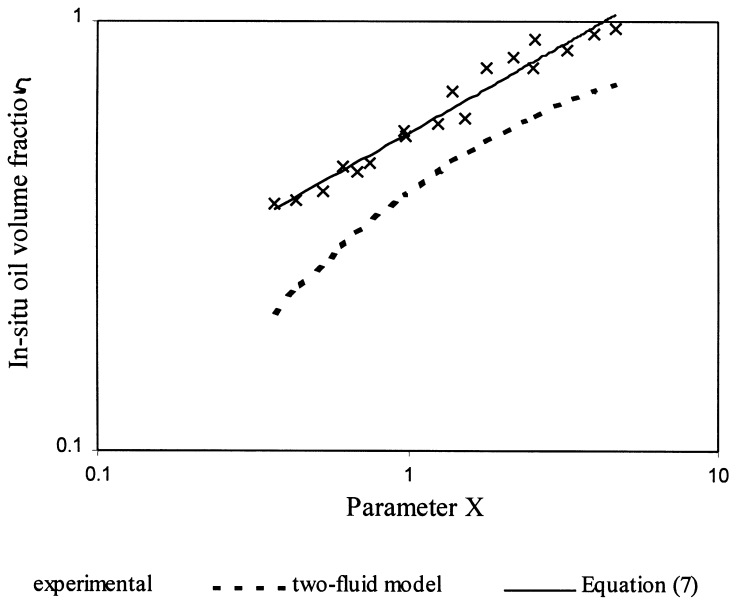

Fig. 18. Comparison of the experimental in-situ oil volume fraction with the predictions of the two-fluid model in the acrylic pipe.

effective in augmenting visual and high speed video observation in clarifying the boundaries of the various flow regimes.

- The flow patterns observed were broadly similar to those defined by previous investigators, though there were substantial differences in the conditions under which they occurred. It was found helpful to define a new intermediate regime, namely Three Layer (3L) flow in which a mixed layer occurred between the water and oil layers at the bottom and top of the pipe respectively.
- There are substantial differences in flow pattern and phase distribution between the acrylic resin (Transpalite^{TM}) and the stainless steel tubes. In the stainless steel tube the propensity for dispersion was greatly increased; in the acrylic tube oil tended to be the continuous phase for a wider range of flow conditions than in the steel tube. Since acrylic resin pipes are widely used in experimental studies of liquid–liquid flows, care should obviously be taken in applying the results of such experiments to practical cases where steel pipes are most widely used.
- The data for in-situ oil volume fraction ε_o correlated well in terms of the Lockhart–Martinelli parameter X. The predictions of the two-fluid model though were lower than the experimental values for ε_o, reflecting perhaps the inadequacy of this model to handle flows which are not completely separated.

Acknowledgements

The authors would like to express their gratitude to Norsk-Hydro a.s. for their contribution

towards the construction of the experimental rig and to Schlumberger Cambridge Research Ltd for the provision of (and advice on) the high frequency probe. P. Angeli is also grateful to Norsk-Hydro for providing financial support during this work.

References

Angeli, P. 1996. Liquid-liquid dispersed flows in horizontal pipes. PhD Thesis, Imperial College, London.

Angeli, P., Hewitt, G.F., 1998. Pressure gradient in horizontal liquid-liquid flows. Int. J. Multiphase Flow 24, 1183–1203.

Arirachakaran, S., Oglesby, K.D., Malinowsky, M.S., Shoham, O., Brill, J.P. 1989. An analysis of oil/water flow phenomena in horizontal pipes. In: SPE Paper 18836, SPE Prod. Operating Symp., Oklahoma, March 13–14, pp. 155–167.

Brauner, N., Moalem Maron, D., 1989. Two phase liquid-liquid stratified flow. PhysicoChemical Hydrodynamics 11, 487–506.

Brauner, N., Moalem Maron, D., 1992. Flow pattern transitions in two-phase liquid-liquid flow in horizontal tubes. Int. J. Multiphase Flow 18, 123–140.

Burgess, J.M., Calderbank, P.H., 1975. The measurement of bubble parameters in two-phase dispersions-I: The development of an improved probe technique. Chem. Engng. Sci 30, 743–750.

Cartellier, A., Achard, J.L., 1991. Local phase detection probes in fluid/fluid two-phase flows. Rev. Sci. Instrum. 62, 279–303.

Charles, M.E., Govier, G.W., Hodgson, G.W., 1961. The horizontal pipeline flow of equal density oil-water mixture. Can. J. Chem. Engng. 39, 27–36.

Guzhov, A., Grishin, A.D., Medredev, V.F., Medredeva, O.P., 1973. Emulsion formation during the flow of two liquids in a pipe. Neft Khoz 8, 58–61 (in Russian).

Hasson, D., Mann, U., Nir, A., 1970. Annular flow of two immiscible liquids. I. Mechanisms. Can. J. Chem. Engng. 48, 514–520.

Hewitt, G.F., 1978. Measurement of Two Phase Flow Parameters. Academic Press, New York.

Jones, O.C., Delhaye, J.M., 1976. Transient and statistical measurement techniques for two-phase flows: a critical review. Int. J. Multiphase Flow 3, 89–116.

Kobori, T., Terada, M. 1978. Application of the needle-type void meter to blow-down test. In: Proc. 2nd CSNI Specialists Meet. on Transient Two-Phase Flow, Paris, pp. 699–714.

Kurban, A.P.A., Angeli, P., Mendes-Tatsis, M.A., Hewitt, G.F. 1995. Stratified and dispersed oil-water flows in horizontal pipes. In: Proc. The 7th International Conference on Multiphase Production, Cannes, France. Mech. Eng. Publications, London, pp. 277–291.

Nädler, M., Mewes, D., 1995. The effect of gas injection on the flow of two immiscible liquids in horizontal pipes. Chem. Engng. Technology 18, 156–165.

Russell, T.W.F., Hodgson, G.W., Govier, G.W., 1959. Horizontal pipeline flow of mixtures of oil and water. Can. J. Chem. Engng. 37, 9–17.

Teyssedou, A., Tapucu, A., Lortie, M., 1988. Impedance probe to measure local void fraction profiles. Rev. Sci. Instrum. 59, 631–638.

Trallero, J.L. 1995. Oil–water flow patterns in horizontal pipes. PhD Thesis, The University of Tulsa.

Valle, A. 1995. Private communication. Norsk Hydro a.s.

Valle, A., Kvandal, H. 1995. Pressure drop and dispersion characteristics of separated oil–water flow. In: Proc. 1st Int. Symp. on Two-Phase Flow Modelling and Experimentation, Rome, Italy, 9–11 October, pp. 583–591.

Valle, A., Utvik, O.H. 1997. Pressure drop, flow pattern and slip for two phase crude oil/water flow: Experiments and model predictions. In: Proc. Int. Symp. on Liquid-Liquid Two Phase Flow and Transport Phenomena, Antalya, Turkey, 3–7 November, pp. 63–74.

van Der Welle, R., 1985. Void fraction, bubble velocity and bubble size in two-phase flow. Int. J. Multiphase Flow 11, 317–345.

Vigneaux, P., Chenais, P., Hulin, J.P., 1988. Liquid-liquid flows in an inclined pipe. AIChE J. 34, 781–789.

Wallis, G.B., 1969. One-dimensional Two-phase Flow. McGraw-Hill, New York.